Hydrochemical Analysis of Groundwater in the Area Northwest of El-Sadat City, West Nile Delta, Egypt

Amal Othman, Hosni Ghazala, and Ismael M. Ibraheem

Abstract The Nile River represents the basic surface water in Egypt as the area beside it is the most fertile land in Egypt. The Nile River's surface has become insufficient in recent years to the Egyptian requirements because of the overpopulation and the recent developing projects' problems. Therefore, searching for new possible reclamation areas turned into a critical need. Intensive efforts have been made to set large agricultural projects and new urban communities in the desert. The study region is located northwest of El-Sadat city (West Nile Delta) covering the area between longitudes 30° 16′ 48″ and 30° 30′ 40″ E and latitudes 30° 21′ 36″ and 30° 31′ 12″ N. It occupies an area of 330 km^2. Because of the presence of such a vital location, a lot of work has been put into developing it. El-Sadat city is one of Egypt's most important new industrial cities. A lot of work has been planned into developing such desired area due to the presence of agricultural soil potentialities, gentle relief, and groundwater resources. The main purpose of the present study is to evaluate the hydrochemical settings of the groundwater and defeat the groundwater shortage problem in this area. The water samples gathered from 57 different drilled water boreholes were tested for the major cations [Mg^{2+}, Ca^{2+}, Na^{+}, K^{+}], major anions [CO_3^{2-}, HCO_3^{-}, SO_4^{2-}, Cl^{-}], Mn and Fe trace elements, in addition to electrical conductivity (EC) and total dissolved solids (TDS). Moreover, the suitability of 57 groundwater boreholes for drinking and irrigation purposes was assessed by comparing with the known standard guidelines' values. Water quality indices such sodium content (SC), sodium adsorption ratio (SAR), residual sodium carbonate

A. Othman (✉) · H. Ghazala
Department of Geology, Faculty of Science, Mansoura University, Mansoura 35116, Egypt
e-mail: osman83@mans.edu.eg

H. Ghazala
e-mail: Ghazala@mans.edu.eg

I. M. Ibraheem
Institute of Geophysics and Meteorology, University of Cologne, Pohligstr. 3, 50969 Cologne, Germany
e-mail: ismael.ibraheem@geo.uni-koeln.de

A. M. Negm and M. El-Rawy (eds.), *Sustainability of Groundwater in the Nile Valley, Egypt*, Earth and Environmental Sciences Library,
https://doi.org/10.1007/978-3-031-12676-5_7

(RSC), permeability index (PI), Kelly's ratio (KI), chloride classification, magnesium hazard (MH), and chloro-alkaline indices were also taken into consideration while assessing the quality of groundwater for agricultural objectives.

Keywords West Nile Delta · El-Sadat city · Water quality · Hydrochemical analysis

1 Overview

The Nile River, as Egypt's principal surface water, aids in boosting the fertility of the land beside the Nile River and around its two branches. These days, the Nile River's surface water got lacking to the Egyptian demands due to the overpopulation issue. The Nile Basin has subjected to several changes in discharge, geomorphology as well as hydrography, since its inception (Gaber et al. 2020). Several efforts have been made to start new urban settlements and enormous agricultural activities in the desert fringe and many researches concern with this issue (Attwa and Ali 2018; El Osta et al. 2018; Gad et al. 2020; Hegazy et al. 2020; McCool 2019; Mohamed 2020; Mosaad and Basheer 2020; Salem et al. 2018, 2019; Salem and Osman 2017).

The main objective of this research is to highlight some information on the quality of the groundwater and its availability and appropriateness for irrigation and human utilities in the region northwest of El-Sadat city in the West Nile Delta. Such current research could be a great informative tool to help constructing new projects concern with establishing new communities and land reclamation purposes. This can help the Egyptian government to implement the desired development strategy for 2030. Groundwater hydrochemistry has a considerable significance concerning the groundwater's suitability for different uses. It helps to assess the hydrochemical processes in charge of the areal changes in the groundwater chemistry (Heath 1983; Miller 1991; Kimblin 1995; Mayo and Loucks 1995; Hudson and Golding 1997; Todd and Mays 2005; Fetter 2014; Şen 2015). As there are several interactions between the earth layers and its surroundings of the atmospheric gasses caused by the man-made materials, no pure water will exist. Therefore, there is an urgent need for groundwater analysis. The hydrochemical analysis deals with the groundwater's chemical composition and its source. In addition, it aims to discover the relation between the rock constitution and the groundwater passing through (Zaporozec 1972). As a result, both the quality and the geological context can be inferred from the groundwater chemical composition (Dauda and Habib 2015). Variations in the geochemistry of the groundwater are commonly used indicators for the aquifer composition variations, because groundwater's geochemistry is a follower of rock mineral composition (Rogers 1989). Ion dissolution results from water circulation in the surrounding soils and rocks. The hydrochemical analysis exhibits to what extent if waters would be suitable for human demands, industrial, and agriculture purposes. This will be carried out through determination of the water type from its constitution, different diagrams, moreover, calculating several indicators helping in taking decision of its suitability for different purposes.

2 Methodology

During many campaigns, water samples were taken directly from boreholes, which are widely utilised for irrigation and drinking. They were collected in pre-cleaned one-liter plastic bottles after a certain pumping duration (exceeding 30 minutes) in order to overcome the contamination and stagnant groundwater problems. The used bottles were washed out numerous times with sampling water, then they were filled and sealed off quickly to avoid being exposed to the air. For identification, each bottle was named and thereafter saved in an icebox container. Within less than three days, the obtained samples were sent to laboratory. A total of fifty seven water samples were collected from different drilled boreholes in the area (Fig. 1). Water samples were subjected to a series of tests to determine the presence of the major anions [CO_3^{2-}, Cl^-, HCO_3^-, SO_4^{2-}], major cations [Mg^{2+}, Ca^{2+}, Na^+, K^+], Fe and Mn trace elements, total dissolved solids, and furthermore electrical conductivity at the Soil Fertility Tests and Fertilizers Quality Control Laboratory, Faculty of Agriculture, Mansoura University, Egypt. Hydrochemical analysis mainly evaluates the different ions concentrations. There are several computer software's that are very useful in the water analysis, especially for large volumes of data with small percentages of error and it would exhibit these data in different manners such as graphs, maps, and tables. Both Rockware AqQA (RockWare Inc. 2004) and Rockwork software have been used to carry out the evaluation of the groundwater data analysis. Graphical presentation of the output of these programs include the most common aqueous geochemistry plots and diagrams, such as Piper and Schoeller charts. These diagrams have a good role in deducing the hydrogeological facies and facilitating data analysis in the investigated region.

3 Geological Settings

Geological and structural settings of the West Nile Delta including the area of interest has been studied by many researchers such as Shata (1953, 1955, 1959, 1961), Zaghloul (1976), Abdel Baki (1983), Shedid (1989), Harms and Wray (1990), Sadek et al. (1990), Abdel Aal et al. (1994, 2001), Sarhan and Hemdan (1994), Sarhan et al. (1996), Garfunkel (1998), Guiraud and Bosworth (1999), Dawoud et al. (2005), ElGalladi et al. (2009), Abd El-Kawy et al. (2011), El Kashouty and El Sabbagh (2011) and Ibraheem et al. (2018).

The surface geology of the West Nile Delta area is represented by Oligocene, Miocene, Pliocene, and Quaternary sediments. Oligocene sediments consist mainly of sandstone, sand, and gravel. These sediments exist at the southwest part of the Nile Delta. Pliocene, Miocene, besides Quaternary deposits consist of sand and sandstones including intercalations of clay and limestone. These deposits are predominant at western and southern parts at Wadi El-Natrun, El Ralat, and Wadi El Farigh depressions, El Washika, Dahr El Tashasha, and Gabel El Hadid (Ibraheem 2009; Ibraheem

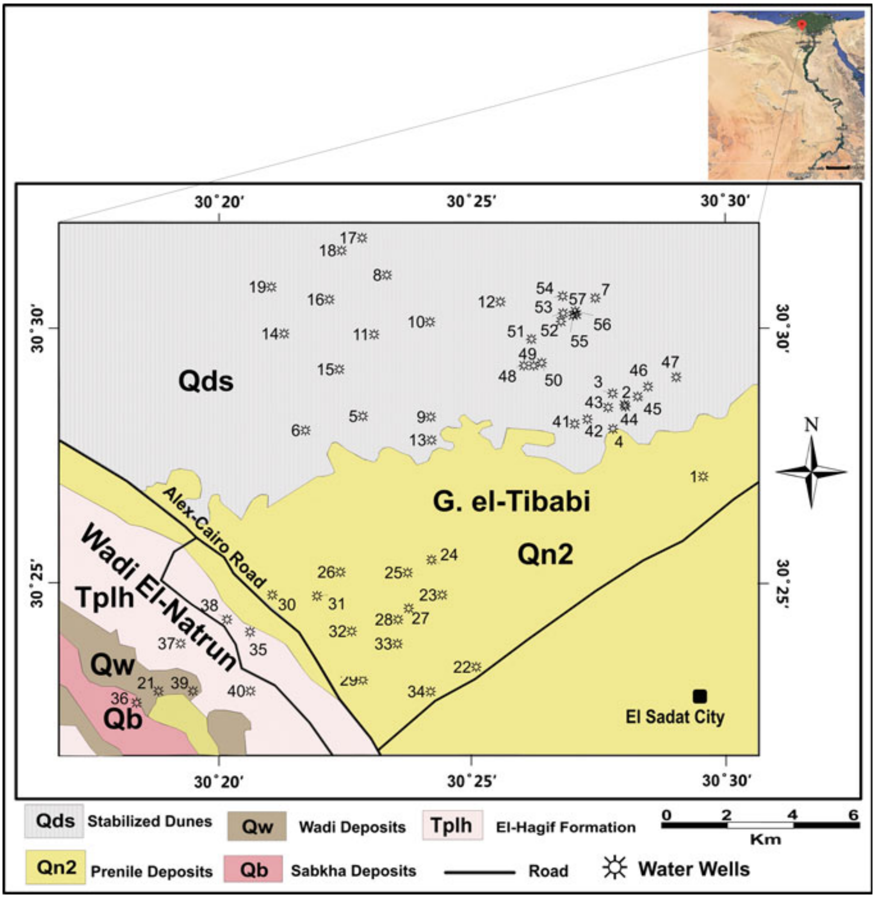

Fig. 1 Groundwater samples' locations posted on the geologic map of the area of interest

et al. 2016). Generally, the studied area is mainly covered by Prenile deposits and stabilized dunes (Fig. 1). The subsurface stratigraphy includes sediments of Quaternary, Pliocene, Miocene, Oligocene, Eocene, Cretaceous, Jurassic, and Triassic ages (Fig. 2). A thick sequence of Late Cretaceous to Quaternary sediments was recorded in the West Nile Delta area (Sharaky et al. 2007).

4 Hydrogeological Settings

Many studies have been carried out on the hydrogeochemical and hydrogeological settings at the area of the West Nile Delta such as: Abdel Baki (1983), Ahmed (1999), Al-Kilany (2001), Embaby (2003), Atta et al. (2005), Dawoud et al. (2005), Ahmed

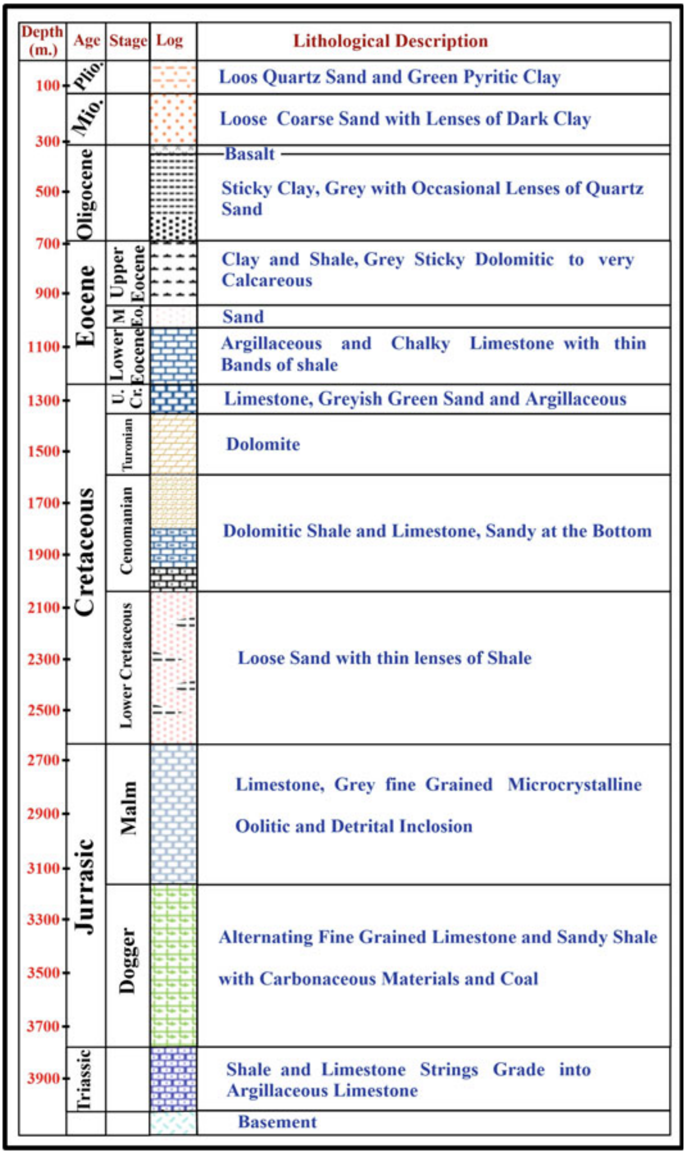

Fig. 2 Stratigraphic column of Sahara Wadi El-Natrun well, Western Desert, Egypt (modified after Ibraheem and El-Qady 2019)

et al. (2011), Massoud et al. (2014), Salem and El-Bayumy (2016), Ibraheem and El-Qady (2017), Abd-Elhamid et al. (2019), Othman et al. (2019), Salem et al. (2019), and Hegazy et al. (2020). They have studied the area of El-Sadat industrial city which is situated to the south of our investigated area and they came to the conclusion that the groundwater in that location is not uniform, with salinity and ionic composition varying. With groundwater movement, the salinity of the groundwater rises gradually from northeastern to southwestern directions. They mentioned also that, as mineralization decreases with depth, this indicates limitations of water penetration to great depths. They claimed that shallow groundwater has high nitrate concentration caused by agriculture procedures and groundwater at northeastern and southwestern parts of industrial areas has high heavy metals concentrations because of the industrial activities. Five different chemical facies (Na–HCO_3, Ca–HCO_3, Na–SO_4, Ca–Cl and Na–Cl) have been recorded at this area indicting process of ion exchange and interactions between the groundwater and the formations.

Salem and El-Bayumy (2016) carried out a study on the groundwater's hydrochemistry of the area east to Wadi El-Natrun. They concluded that most of the groundwater samples are convenient for irrigation purposes except some samples having high EC values. The samples show low to medium salinity and low sodium absorption ratio values. The main groundwater types are: Na–HCO_3, Na–Cl, Ca–HCO_3, Mg–Cl and Mg–HCO_3. Sodium/Chloride/Carbonate water types are dominant at that area. Also, El Osta et al. (2018) discussed the groundwater flow and Vulnerability at the district of Wadi El-Natrun depression and its surroundings using numerical simulation and concluded that the present groundwater over-abstraction has resulted in a general head drawdown of 3 m in 2015 and will reach 40 m in 2050. Moreover, they mentioned that the western parts of their study area have a high vulnerability rate (>110).

Generally, the West Nile Delta area has four main groundwater aquifers: Oligocene, Miocene, Pliocene and Quaternary aquifers.

4.1 Quaternary Aquifer

The first main aquifer in the West Nile Delta is the Quaternary aquifer which is located at the Coastal Plain, the Rolling Plains of the Nile Delta, and Nile Delta floodplain (Geirnaert and Laeven 1992; Mohamed and Hua 2010). It represents the substantial water-bearing zone in the region along east Abu Rawash–Khatatba–El-Sadat–Alexandria where it changes from 100 to 500 m (in thickness) towards the coast. It is composed of sandy and gravely layers. Clay strata split the aquifer into smaller confined sub-aquifers.

Quaternary aquifer is subdivided into Recent aquifer and Pleistocene aquifer. Recent aquifer (sand with some intercalations of aeolian deposits) is predominant at the depression of Wadi El-Natrun (Ibraheem 2009). The main groundwater unit of the Pleistocene deposits is Sahl El-Tahrer which is remarked by the presence of Pliocene sediments at its base (Menco 1990). The Nile Delta groundwater is the main recharger for the Pleistocene aquifer at El-Sadat area. There are other water source supplies by seepages from the irrigation canals and/or cultivated lands, and strong rainstorms. Pleistocene deltaic deposits compose the main Nile Delta aquifer. These deposits consist of unconsolidated coarse sands and gravels with the existence of lenses, and it covers a thick clay layer of Pliocene age (Sherif 1999).

4.2 Pliocene Aquifer

Omara and Sanad (1975) mentioned that Pliocene aquifer is made up of multi layers of sand and clay. It is subdivided into two parts: the lower part consists of sandy horizon with thickness varying from 1 to 10 m, while the upper part is made up of loose sand and sandstone with a thickness of 15 m. Between the two parts, there is a thick clay bed, so that the groundwater at the lower part is found under confined condition. The Upper part is found in a semi-confined condition due to the existence of layers of sandy clay above it.

4.3 Miocene Aquifer

Miocene (Moghra Fm.) aquifer is the second main aquifer in the West Nile Delta. Dawoud et al. (2005) mentioned this aquifer as well developed at Wadi El Farigh and has a variable thickness (50–250 m). This aquifer is mainly sand, sandstone, and clay interbeds with silicified wood and vertebrate remains (Said 1962).

4.4 Oligocene Aquifer

Oligocene aquifer is found at the western parts of Cairo. It consists of gravel, sand, thin bands of limestone and clay interbeds (Salem and El-Bayumy 2016). Both rainwater and paleowater are the main recharge sources for this aquifer (Abdel Baki 1983; El Abd 2005).

5 Results

5.1 Numerical Water Quality Indicators

Water classification based on different combinations of the major ions can provide water quality indicators representing guidelines for assessing the groundwater

Table 1 Classification of water according to EC, TDS and TH

Parameter	Classification		References
TDS (mg/L)	0–1000	Fresh	Fetter (2014)
	1000–10,000	Brackish	
	10,000–100,000	Saline	
	>100,000	Brine	
EC (µS/cm)	<250	Excellent	Wilcox (1955) and Şen (2015)
	250–750	Good	
	750–2000	Permissible	
	2000–3000	Doubtful	
	>3000	Unsuitable	
Hardness (mg/L)	0–75	Soft	Şen (2015)
	75–150	Moderately hard	
	150–300	Hard	
	>300	Very hard	

quality. The classification of groundwater according to total dissolved solids (TDS), electrical conductivity (EC), and total hardness (TH) is given in Table 1.

5.1.1 Electrical Conductivity (EC) and Total Dissolved Solids (TDS)

Electrical conductivity and total dissolved solids are the most commonly calculated physical parameters. TDS is known as the total quantity of the solids especially the inorganic one existing in the water. High concentrations of TDS would affect negatively both soil and crops by reducing the groundwater's suitability for the human utilities and irrigation supply. TDS levels in water samples are significantly associated with the rock weathering process and many other factors (Jacks 1973; Rao 2002; Bartarya 1993).

Electrical conductivity is defined as the water ability to pass the electrical current and it helps to study the groundwater's quality. High EC values may result in a gastrointestinal irritation for consumers (World Health Organization [WHO] 2011). Groundwater having high EC levels are unsuitable for both domestic and irrigation utilities.

Figure 3a, b exhibit the distribution maps of TDS and EC of the surveyed area. They exhibit a zone of high EC and TDS levels at the northwestern sector of the study area. The TDS and EC of the water samples have a clear linear relationship shown in Fig. 4. The following empirical formula illustrates the relationship between TDS and EC (Walton 1989):

$$\text{TDS}\ (\text{mg/L}) = \delta \text{EC}\ (\mu\text{s/cm}) \tag{1}$$

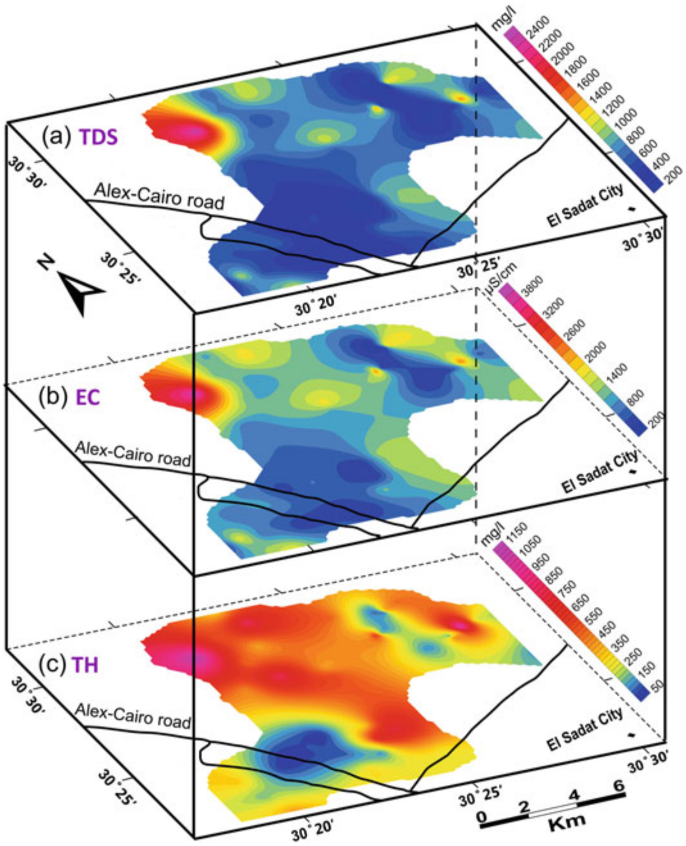

Fig. 3 A map showing the spatial distribution for **a** TDS, **b** EC, and **c** TH

The parameter δ was computed for the water samples in the area of interest as it equals 0.625, therefore the formula can be expressed by Eq. 2:

$$\text{TDS} = 0.625\,\text{EC} \quad (2)$$

5.1.2 Total Hardness (TH)

Hardness is taken into account as a crucial property for domestic and industrial classification of water quality. It depends mainly on the presence of magnesium (Mg^{2+}) and calcium (Ca^{2+}) and it is estimated in milligram per liter (Şen 2015). The following equation expresses the total hardness in terms of the calcium carbonate equivalent (Todd and Mays 2005).

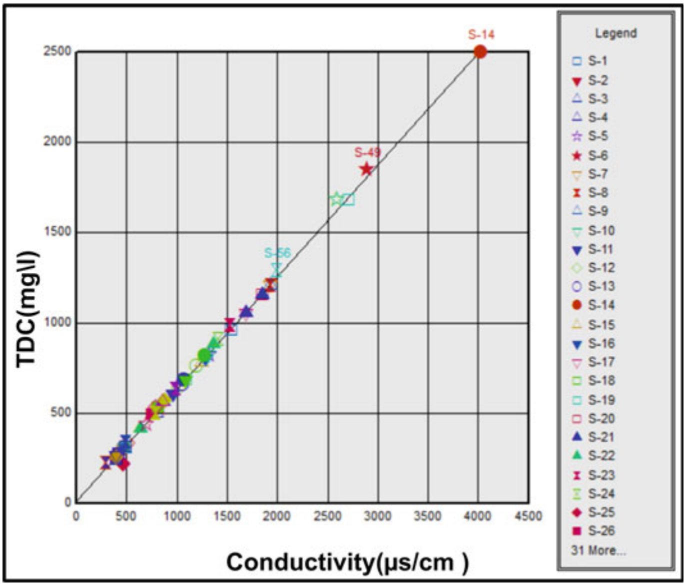

Fig. 4 Linear cross plot between TDS and EC for the gathered water samples in the study area

$$TH = 2.5\left[Ca^{2+}\right] + 4.1\left[Mg^{2+}\right] \quad (3)$$

as TH, $[Mg^{2+}]$ and $[Ca^{2+}]$, are in mg/L.

For domestic purposes, if hardness exceeds 200 mg/L, then it would affect the water taste and may form a dirty layer of the groundwater (scum formation) (Burbery and Vincent 2009). The total hardness has been calculated for the water samples (Fig. 3c). High TH levels can be seen at the surveyed area except at the southwestern part in addition to other places at the eastern part of the region.

5.2 Groundwater Hydrochemical Analysis

Major ions existing in the groundwater samples are controlled by several factors such as climate conditions, rock nature and the movement ability of water. Both variable nature and the human activity are obvious through the differences in the hydrochemical parameters (Karanth 1991). Surface and subsurface physicochemical conditions usually affect the ion distribution (Aghazadeh and Mogaddam 2010).

Water chemical parameters include different ions concentrations: major anions (Cl^{-}, SO_4^{2-}, HCO_3^{-} and CO_3^{2-}) and major cations (Na^{+}, K^{+}, Ca^{2+}, and Mg^{2+}). A summarize of the maximum, minimum, average, and standard deviation for different chemical parameters obtained in our study is shown in Table 2. Figures 5 and 6 represent a graphical representation for exhibiting the different concentrations of both cations and anions.

Table 2 Physicochemical parameter statistics

Parameter	Minimum value	Maximum value	Average value	Standard deviation
Na^{+}	2.9	329.4	117.9	90.71
K^{+}	0	9	6.2	2.15
Mg^{2+}	0	122.7	24.5	18.54
Ca^{2+}	0	418	113.5	88
HCO_3^{-}	7.2	585.6	227.5	113.3
CO_3^{2-}	0	27.7	2.38	5.83
Cl^{-}	20	630.9	159	144.5
SO_4^{2-}	0	930	228	180.8
EC	300	4032	1127	734.6
TDS	216.2	2500	709	458.9

All previous parameters are measured in mg/L unless EC in μS/cm

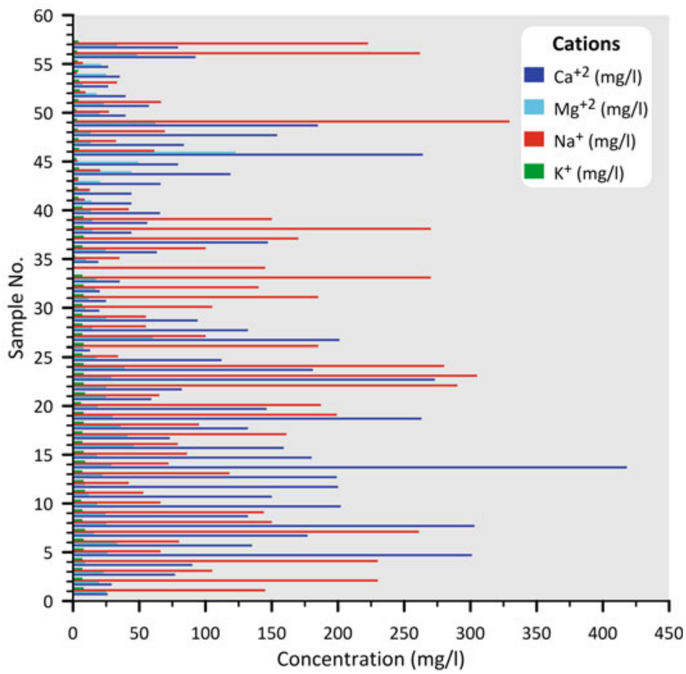

Fig. 5 The concentrations of various cations for the gathered groundwater samples

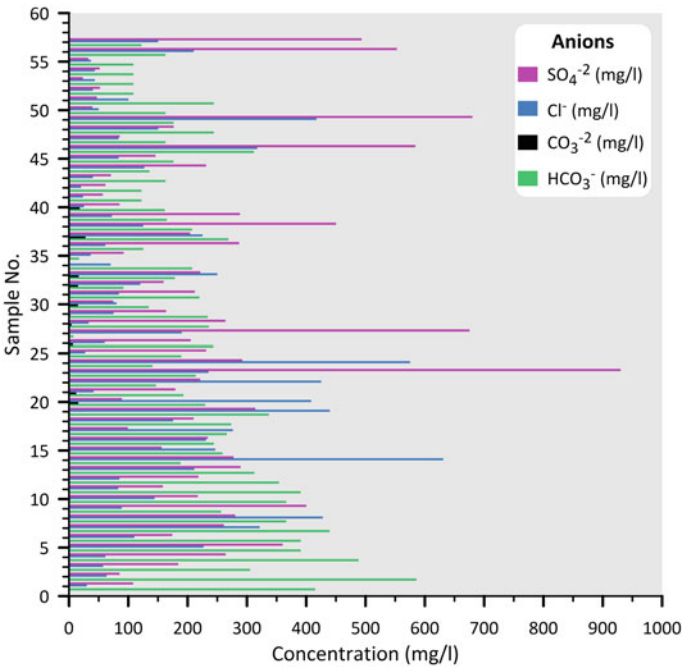

Fig. 6 The concentrations of various anions for the collected groundwater samples

5.2.1 Major Cations

Calcium (Ca^{2+}) and Magnesium (Mg^{2+})

In boilers and other heat exchange equipments, magnesium and calcium cations interact with sulphate, carbonate, bicarbonate, and silica to produce a heat-retarding, pipe-clogging scale. Moreover, they combine with fatty acid ions in soaps to generate soapsuds, therefore the higher the calcium and magnesium content, the greater the need for soap to form suds (Heath 1983).

Calcium content changes from 0 mg/L at well 34 to 418 mg/L at well 14. It could be concluded that about 58% of all water samples are considered natural waters, as calcium concentrations don't exceed 100 mg/L (Todd and Mays 2005). The spatial distribution map (Fig. 7a) representing the existing calcium cation exhibits high values at the northwestern sector of the region, moderate values in the centre of the area towards northwest-southeast direction, and low levels at the eastern and southwestern parts of the study region. This map shows a good harmonization with the total hardness distribution map (Fig. 3c).

High content of magnesium cation has laxative effect especially on the supply's new users (Todd and Mays 2005). It also has a side effect on the soil causing alkaline environment and hence lowering the crops product. Magnesium levels change from

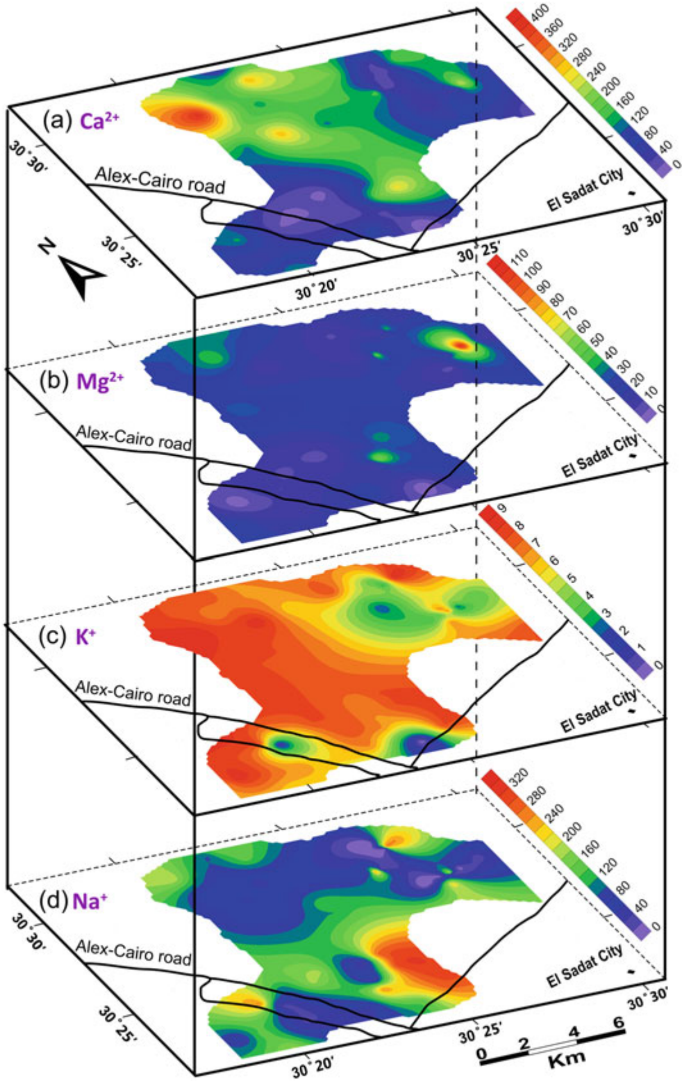

Fig. 7 The major cations' spatial distribution maps

0 mg/L at well 34 to 122.7 mg/L at well 46 and has 30.6 mg/L as an average value. The distribution map of Mg^{2+} shows high Mg^{2+} concentration zone at the northeast portion (Fig. 7b). Based on Todd and Mays (2005), all water samples are considered to have natural magnesium concentration except three groundwater samples (at wells 27, 46, and 49). These samples have Mg^{2+} concentration exceeding 50 mg/L.

Groundwater equilibrium state is well related to the existence of Ca^{2+} and Mg^{2+} cations in water (Negm and Armanuos 2017). Concentrations of these two cations in natural waters differ over a wide range relying on the history of the water sample including the geochemical characteristics and the geological formations (Şen 2015). Mg^{2+} and Ca^{2+} are very similar in several aspects and they could be dissolved from different soils and rocks (Salomons and Forstner 1984). Mg^{2+} and Ca^{2+} cations distribution maps indicate that the majority of the research area has low concentrations of both magnesium and calcium except some small zones.

Potassium (K^+)

Most natural waters have K^+ levels less than 10 mg/L (Chow 1964). K^+ cation is similar to Na^+ in many aspects but differs in other manners affecting its existence in water and its effect on other utilities (Şen 2015). All of the samples in the research area have K^+ concentration below 10 mg/L where K^+ concentration changes between 0 and 9 mg/L with an average value of 6.23 mg/L. The aerial distribution map of potassium level (Fig. 7c) reveals normal K^+ levels all over the study area. These normal K^+ levels are probably due to the nature of the sediments constituting the aquifer as potassium salts are insoluble in several types of rocks (Sharaky et al. 2017).

Sodium (Na^+)

Sodium is a wide common alkali metal in the natural water that is linked to the salinity of the groundwater (Ghoraba and Khan 2013). Existence of high concentration of Na^+ cation would be resulted from several factors such as rock weathering and ion exchange reactions (Stallard and Edmond 1983; Stimson et al. 2001). Chemical analysis of the sodium relative to the total cations is important in case of cation exchange process in sediments (Zaporozec 1972). Under normal cases, groundwater includes Na^+ and Cl^-. In the current study; Na^+ concentration differs from 2.9 mg/L as a minimum value at borehole no. 54 to 329.4 mg/L at borehole no. 49 with an averaged value of 116.11 mg/L. There are eleven samples of the groundwater having concentrations exceeding 200 mg/L, while the rest have acceptable values. Hence, it could be considered as natural water and is suitable for domestic purposes. Figure 7d shows the spatial distribution map of Na^+. This map highlights four high Na^+ zones in the northeast, southeast, northwest, and western sectors of the area under investigation. This may be a result from the fertilizers used for agricultural purposes. In the presence of suspended particles, salt and potassium concentrations greater than 50 mg/L create foaming, which increases scale formation and corrosion in boilers (Todd and Mays 2005). High concentration of sodium would also cause cardiac problems, hypertension, and other medical difficulties. Depending on the presence of calcium and magnesium concentrations in water, sodium would be harmful to certain irrigated crops (Heath 1983).

5.2.2 Major Anions

Bicarbonate (HCO_3^-) and Carbonate (CO_3^{2-})

Concentrations of carbonate (CO_3^{2-}) and bicarbonate (HCO_3^-) are related to the value of the PH and they could be described as the total alkalinity (Fetter 2014). They control the water capacity to neutralized strong acids (Heath 1983). Concerning HCO_3^-, the minimum concentration is 7.2 mg/L, while the highest value is 585.6 mg/L with a value of 225.3 mg/L on average. Groundwater samples in the research region have normal HCO_3^- levels (less than 500 mg/L), except the sample no. 2 which has high value (585.6 mg/L). The spatial distribution map of HCO_3^- (Fig. 8a) shows two relatively high-level zones in the eastern parts, while moderate values are found at the northwestern parts, and low levels are encountered at the southern zones of the study area, but mostly in permissible levels. Bicarbonates of magnesium and calcium dissolve in the water heater to form scale and emit corrosive carbon dioxide gas (Heath 1983).

Percolation process for the waters enriched in CO_3^{2-} resulting from the dissolution of the carbonate rocks with the aid of atmosphere increase the bicarbonate concentration and led to the existence of Ca–HCO_3 groundwater type (Edmunds et al. 1987; Appelo and Postma 1996). CO_3^{2-} is found in the water samples with a value of 2.34 mg/L on average, with the highest value of 27.7 mg/L at borehole no. 37, whereas the minimum value is zero mg/L. Only six water samples have CO_3^{2-} concentration more than 10 mg/L, and the rest of water samples in the area have normal levels and suggest natural waters suitable for domestic purposes. The spatial distribution map of CO_3^{2-} is well presented in Fig. 8b that appears to have two high CO_3^{2-} level sectors in the southwestern parts of the research area.

Chloride (Cl^-)

Groundwater content of chloride initiates from natural and anthropogenic origins (Sayyed and Bhosle 2011). Gradually, Cl^- concentration could be high because of leaching of the saline residues from the sediments (Patil et al. 2020). Moreover, it might be related to included NaCl fluid and by atmospheric deposition. Human activities also result in the Cl^- ions existence in the groundwater (Rogers 1989). The threshold value of Cl^- in groundwater is 250 mg/L (WHO 2011), therefore samples exceeding this limit would have salty taste when chloride combines with sodium. Water would be described as corrosive water in case of high concentration of chloride (Heath 1983). Concentration of Cl^- is very important in case of agricultural activities as it is mostly absorbed by plants. Cl^- is a good guide for groundwater chemical processes. Low Cl^- levels indicate freshwater entrance into the aquifer, while high Cl^- concentrations might be resulted from different process of saline water intrusion, solid salts solutions from the rocks, and evapotranspiration (Şen 2015).

Chloride anion is found with different concentrations in the obtained water samples, as it changes from 20 mg/L at well no. 42 to 630.92 mg/L at borehole no. 14, and has average value of 157.312 mg/L. Cl^- aerial distribution map (Fig. 8c) shows several zones with high Cl^- levels at different parts of the region; northeast,

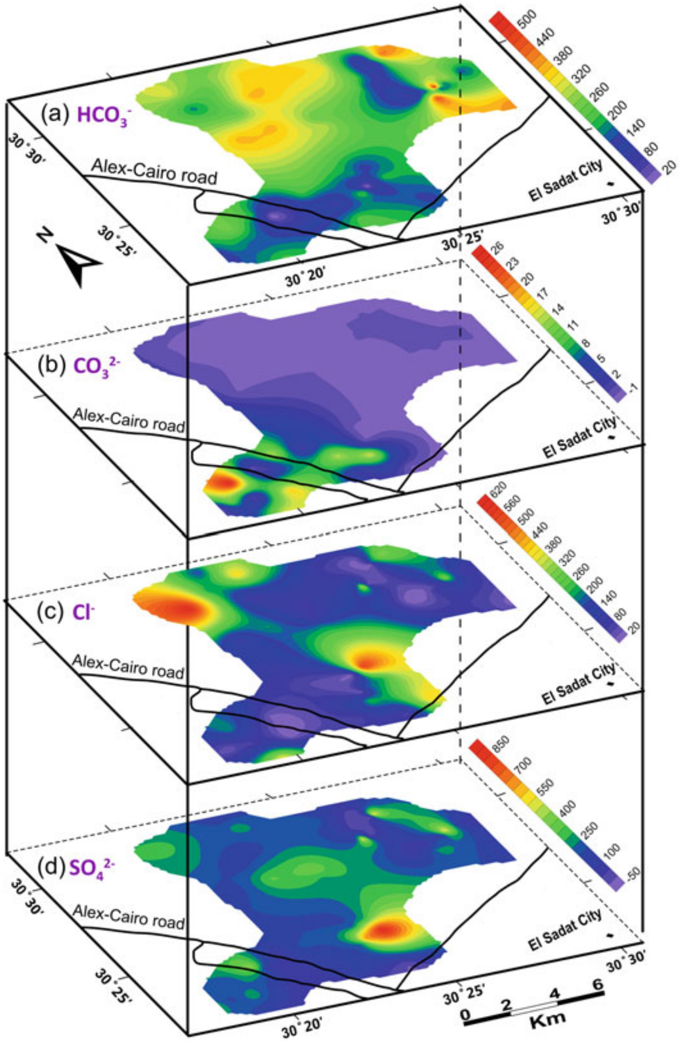

Fig. 8 The major anions' spatial distribution maps

northwest, southeast and western parts, whereas the central part has low Cl^- concentrations. There is a good consensus between the spatial distribution maps of Na^+ and Cl^-. High levels of Cl^- exceeding 350 mg/L would be harmful to the agricultural crops (Hopkins et al. 2007), and this was observed only in 6 groundwater samples (8, 19, 20, 22, 24, and 49).

Sulfate (SO_4^{2-})

The SO_4^{2-} levels usually increase with the salinity of the water samples. It could result from the interaction between water and gypsum presents in the Pleistocene sediments (Atta et al. 2005). An existence of SO_4^{2-} could be caused by pyrite oxidation, gypsum dissolution and/or by barite, especially in sedimentary bedrock areas (Rogers 1989). The maximum SO_4^{2-} level in fresh groundwater is 1360 m/L (Şen 2015), therefore all water samples have acceptable concentrations of SO_4^{2-} anions. SO_4^{2-} content fluctuates from zero mg/L at borehole no. 34 to 930 mg/L at borehole no. 23 as a maximum value. In accordance with (Heath 1983), presence of sulfate with certain concentrations (300–400 mg/L) results in a bitter taste, while at higher concentrations (600–1000 mg/L) it provides a laxative effect. So, we can deduce that only 12.2% of all samples gives a laxative effect and the rest of samples show bitter taste. Figure 8d presents the SO_4^{2-} distribution map in the study area. It reveals only one high SO_4^{2-} zone in the southern part, while almost the whole area has permissible levels of SO_4^{2-}.

5.2.3 Trace Elements

Secondary concentrations of trace elements were identified in the studied groundwater samples. The acceptable drinking water limits are 0.1 and 0.3 mg/L for manganese and iron, respectively (WHO 2011). The concentration of manganese ranges from 0.05 and 0.96 mg/L. The map representing the spatial distribution of manganese clarifies exceeding the permissible guideline value in the surveyed area unless the central and the western parts (Fig. 9a). Iron level differs from 0.01 mg/L at borehole no. 15 to 1.12 mg/L at borehole no. 12 with a value of 0.361 mg/L on average. Iron spatial distribution map shows two high iron level zones in the study region (Fig. 9b). The existence of iron and manganese is an indicator that the groundwater quality is reduced (Burbery and Vincent 2009). Although these ions (Fe^{2+} and Mn^{2+}) are useful for stain laundry, they are harmful in food processing, ice manufacturing, bleaching, brewing, dyeing, and different industry process (Heath 1983).

5.3 Water Quality Graphical Representation

Water quality could be analyzed by graphical representation of different ions existing in water. This method of analysis is quick, easy, effective, and informative way to understand water quality and to decide groundwater's convenience for different intents (drinking, domestic, agricultural, or industrial), so it enhances and manages drilling new wells. The graphical representation includes Schoeller, Piper's tri-linear and Durov diagrams.

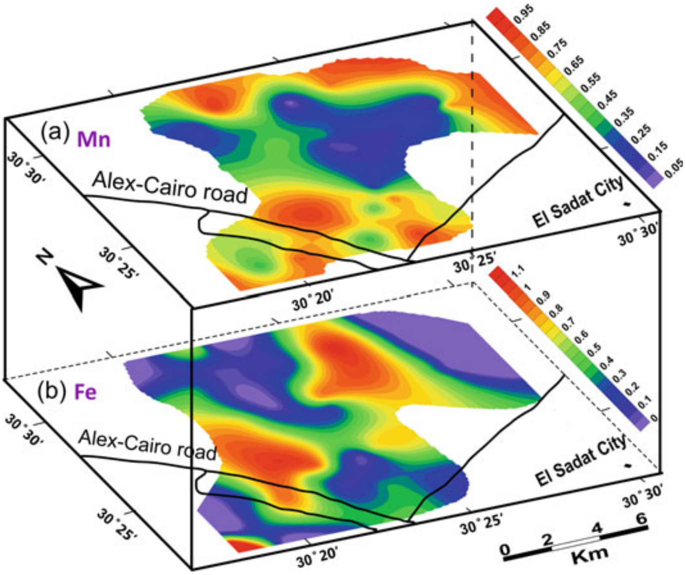

Fig. 9 Spatial distribution maps of concentrations of trace elements of **a** Mn^{2+} and **b** Fe^{2+} at the research area

5.3.1 Schoeller Diagram

Schoeller diagram is a semi-logarithmic graphic with eight vertical logarithmic scales that are evenly spaced representing several ions concentrations in equivalents per million (Schoeller 1967). Applying the logarithmic scale for this diagram is to distribute the appearance of the concentrations as it amplifies low concentrations and decreases high levels. All ions concentrations are plotted as points for each sample then a straight line tied them. This diagram reveals the absolute concentration of each ion and the difference between samples. This diagram evaluates the saturation degree of groundwater with both of calcium carbonate and calcium sulfate (Şen 2015). Moreover, it could describe the average chemical composition of the samples (Ghoraba and Khan 2013). Schoeller diagram represented in Fig. 10 has been sketched for all gathered groundwater samples in the region of the investigation using Aq.QA® software. It reveals that the general trend of ions in mg/L exposes $Ca^{2+} > Na^{+} > Mg^{2+} > K^{+}$ and $HCO_3^{-} > Cl^{-} > SO_4^{2-} > CO_3^{2-}$.

5.3.2 Piper's Tri-Linear Diagram

Piper diagram is another graphical representation which achieves the combined effect of major constitutes of water controlling its quality in a single diagram (Şen 2015). It explains different variables related to the major cations and anions and reveals the main chemical components of the waters. It also shows both similarities and

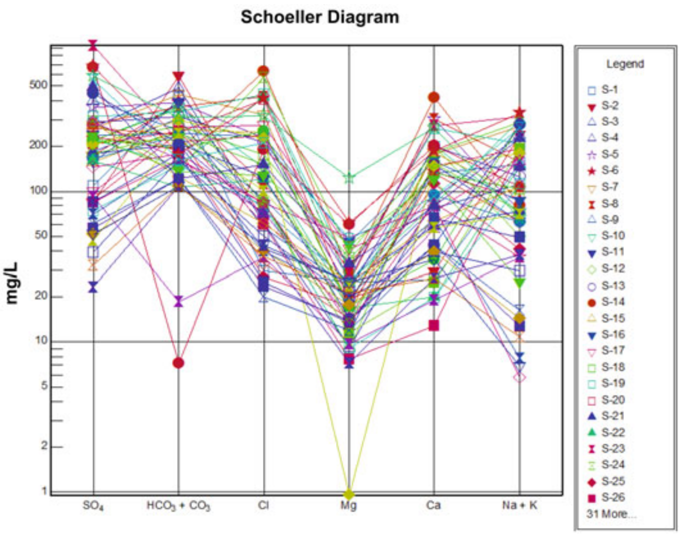

Fig. 10 Schoeller diagram representing all water samples in the study area

differences between samples of water (Piper 1944, 1953). Piper diagram represents a powerful technique in chemistry analysis of the groundwater (Dauda and Habib 2015). It is made up of a rhombus and two triangles. Each triangle represents three ion concentration percentages. The rhombus form depicts the composition of water in terms of cations and anions (Fetter 2014). Piper's tri-linear diagram is a good analytical and representative way to illustrate the classification of the main chemical components and hydrochemical facies of the waters within the area. Aq.QA® computer software has been used to establish the Piper diagram for the collected water samples (Fig. 11).

The triangle corresponding cations reflects a percentage of 42.12% of the existing water samples is of calcium type, moreover, sodium and potassium type represents 33.33%, while 24.56% of the samples showed no sign of a dominating type. Furthermore, the triangle demonstrating anions suggests that 45.61% of the water samples did not display any dominant element, 22.82% represents a type of bicarbonate, 19.29% reflects sulfate type, and chloride type has a percentage of 12.28%. Furthermore, 66.7% of the water samples are on the left side of the diamond demonstrating the alkaline ($Ca^{2+} + Mg^{2+}$) predominance over alkalies earth ($Na^{+} + K^{+}$), whereas the right side of the rhombus is filled with 33.3% of the samples and suggests that alkalies prevail over alkaline earth. Also, groundwater's strong acids ($SO_4^{2-} + Cl^{-}$) representing 77.2% exceed week acids ($CO_3^{2-} + HCO_3^{-}$) whereas the left over samples (22.8%) demonstrate that strong acids are overcome by weak acids. Besides, mixed water type is found in 43.86% of groundwater samples, sodium-chloride type corresponds 26.33% of the samples, 15.78% show magnesium-bicarbonate type, while calcium-chloride type is represented by 10.52%, and lastly 3.53% are of sodium-bicarbonate type. Figure 12 shows the geographical distribution for the different

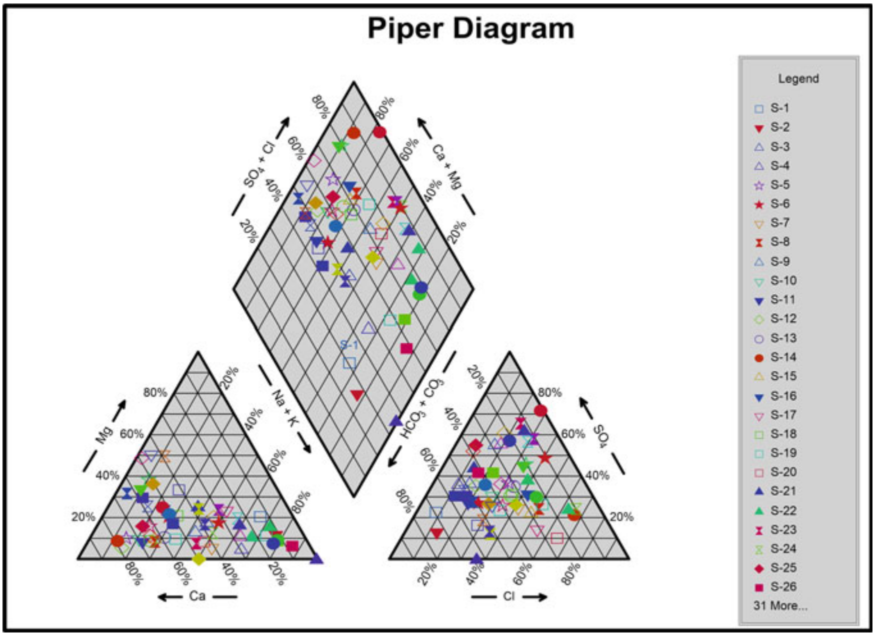

Fig. 11 Piper diagram represents the groundwater samples' hydrogeological facies at the area of interest

hydrochemical types according to Piper tri-linear scheme in the study region. It reveals that the mixed water type is located at northern, central and southwestern parts of the area. While, CaCl type is found at northern locations and this is related with relatively high concentrations of calcium cations which may be dissolved from different rocks and soils. On the other hand, NaCl type is dominant at the southern parts of the area. This could be caused by agriculture activities effect and/or ion exchange reactions. Moreover, $MgHCO_3$ water type characterizes the northeastern parts of the research region corresponding to high concentrations of Magnesium cations.

5.3.3 Durov Diagram

Another hydrochemical graphical representation could be carried out by Durov diagram which has been constructed by Durov (1948). Generally, it relies on the percentages of each cation and anion in milliequivalent. It is made of two ternary charts. Both anions and cations are plotted in separate triangles, then by extending points with lines to intersect, the resultant point in the central rectangle reflects the water type. Durov diagram plays a crucial function in determining the concentration, the origin of the groundwater chemical ingredients, and the total dissolved solids. A code has been provided by Al-Bassam et al. (1997) to process data using Durov

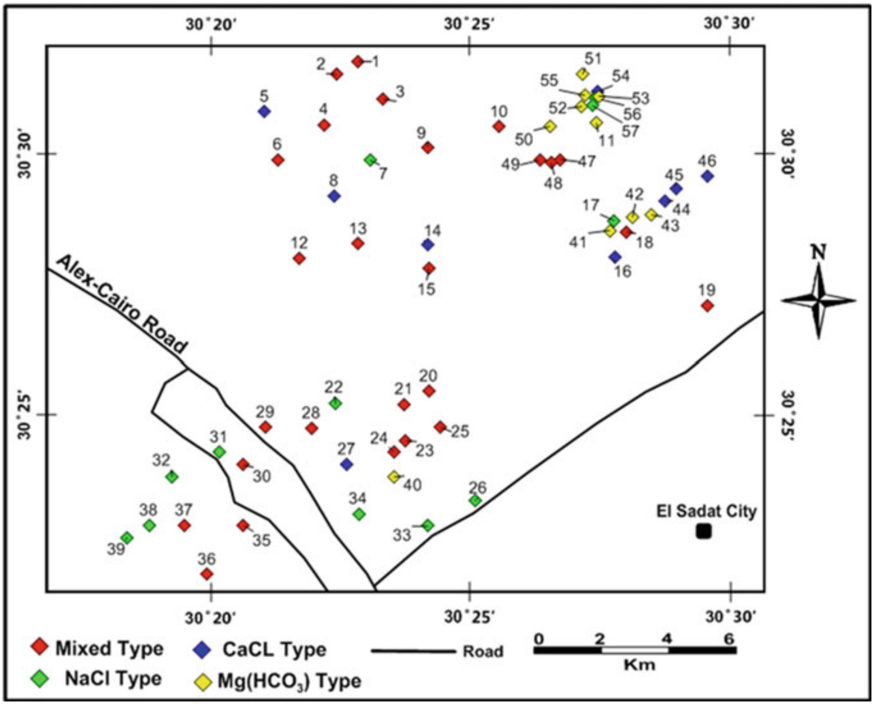

Fig. 12 The spatial distribution map representing the different hydrochemical water types revealed from Piper's tri-linear diagram

diagram. This diagram may give more information about the hydrochemical facies of the groundwater by defining its type or provide some useful geochemical processes for more understanding and analyzing the quality of the groundwater (Ghoraba and Khan 2013). Analyzing Durov diagram according to groundwater classification based on this diagram (Lloyd and Heathcote 1985) reveals that more than 61% of water samples are in a simple dissolution or mixing phase with no dominant anion or cation. Durov diagram exhibits that the mixed water type in the current region are found at field 5 (61% of all groundwater samples) along the mixing or dissolution line. The trend of this line may be related to the recent fresh water recharge indicating little dissolution or mixing with no dominant cation or anion (based on Lloyd and Heathcote 1985). While about 18% of all water samples are at field 2 that suggests the water type is characterized by Ca and HCO_3 with the presence of Na. These waters are affected by ion exchange. Moreover, a percent of 12% of the groundwater samples is located at field 8 reveals that these water types are dominated with Cl and Na and assumes that the groundwater is affected with the process of reverse ion exchange of Na–Cl waters. Furthermore, the rest of samples are dominant with HCO_3 and Ca, SO_4, Cl and Na, and SO_4 and Na (Fig. 13).

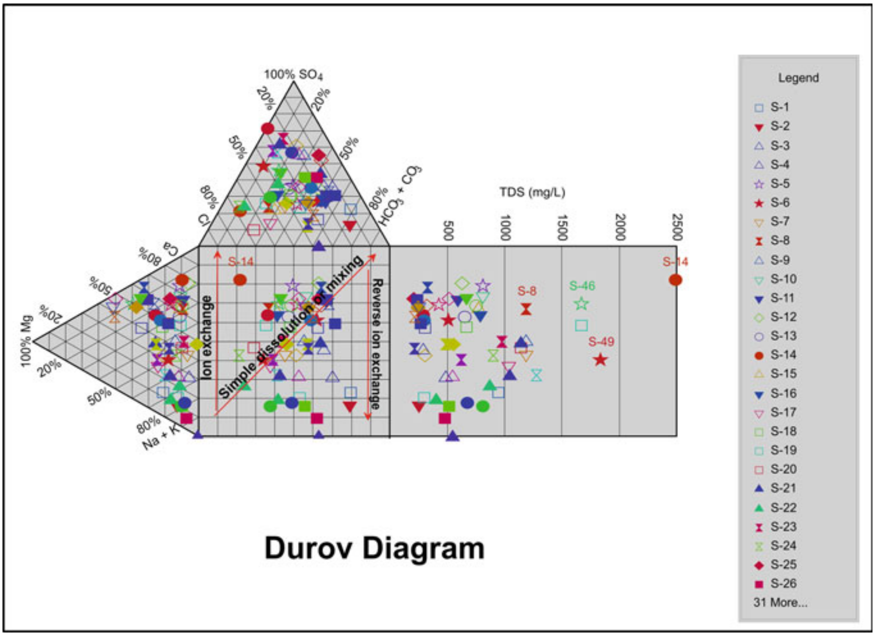

Fig. 13 The gathered groundwater samples are depicted in a Durov diagram drawn using Aq.QA® computer software (RockWare Inc. 2004)

6 Suitability of Groundwater for Irrigation Purposes

Groundwater suitability for irrigation purposes relies on the TDS concentrations which in turn have a high affect on both productivity and quality of crops. Groundwater quality could be decided based on different indicators like sodium content (SC), permeability index (PI), sodium adsorption ratio (SAR), residual sodium carbonate (RSC), Kelly's ratio (KI), magnesium hazard (MH), chloro-alkaline Indices (CAI), chloride classification, and corrosively Ratio (CR), as shown in Tables 3 and 4. Figure 14 represents bar chart plots revealing several parameters of water quality in the investigated area.

6.1 Sodium Content (SC)

Sodium ion concentration has a negative impact on the crop yield, which is reduced when Na^+ enters the vacuum areas in the soil causing a decrease in permeability (Şen 2015). Therefore, SC represents a very significant index. SC could be obtained by expression (Eq. 4).

Table 3 Classification of water quality

Parameter	Classification		Reference
SC (%)	<20	Excellent	Wilcox (1955)
	20–40	Good	
	40–60	Permissible	
	60–80	Doubtful	
	>80	Unsuitable	
SAR (epm)	<10	Excellent	Todd and Mays (2005) and Şen (2015)
	10–18	Good	
	18–26	Permissible	
	>26	Doubtful	
RSC (meq/L)	<1.25	Safe for drinking	Eaton (1950) and Richards (1954)
	1.25–2.50	Marginal as an irrigation source	
	>2.5	Unsuitable for irrigation without amendment	
MH	<50%	Suitable	Negm and Armanuos (2017)
	>50%	Unsuitable	
PI	>75%	Class-I	Doneen (1962)
	25–75%	Class-II	
	<25%	Class-III	

$$SC\ (\%) = 100 * \frac{\left(Na^{+} + K^{+}\right)}{(\mathrm{Ca}^{2+} + \mathrm{Mg}^{2+} + \mathrm{Na}^{+} + \mathrm{K}^{+})} \quad (4)$$

6.2 *Sodium Adsorption Ratio (SAR)*

Both water salinity and SAR are good indicators for groundwater suitability for irrigation. This is depending on sodium concentration that impacts the soil and hence the permeability. SAR evaluates the hazard of Na^+ to agricultural crops and is obtained by Eq. 5, after converting mg/L unit into meq/L unit (Todd and Mays 2005).

$$SAR = \frac{Na^{+}}{\sqrt{\frac{Ca^{2+}+Mg^{2+}}{2}}} \quad (5)$$

It reflects the ability of the soil to absorb Na^+. At high values of SAR, the soil must be adapted to avoid long term disturbances. SAR calculation is important due to Na^+ displacement phenomenon with both Ca^{2+} and Mg^{2+} in the same soil resulting

Table 4 Water quality classification depending on a variety of indicators

Sample number	EC	TDS	SC	PI	SAR	RSC	Hardness	CAI	KI	CR	MH
1	1548	960	65.81	92	4.85	3.42	167.5	−6.66906	1.86	0.52	61.57
2	419	260	76.8	100.18	8.07	6.52	152.45	−4.62177	3.25	0.46	52.84
3	484	300	45.14	65.83	2.69	−0.77	286.8	−1.89131	0.79	1.26	33.23
4	806	500	65.93	84.07	6.17	2.74	262.39	−4.80312	1.9	1.023	14.44
5	1323	820	15.15	26.88	0.98	−10.82	859.1	0.527539	0.17	2.65	12.58
6	839	520	27.94	46.3	1.6	−3.1	472.8	−0.16668	0.37	1.28	28.94
7	1935	1200	53.27	65.24	5.04	−2.96	506.87	−0.25535	1.12	2.59	12.87
8	1935	1200	28	37.77	2.22	−11.23	860	0.454261	0.38	3.9	12.08
9	1935	1200	42.75	55.83	3.02	−4.42	429.63	−1.52922	0.73	2.92	23.47
10	1323	820	20.68	36.76	1.19	−5.6	578.8	0.268107	0.25	1.75	12.93
11	968	600	23.04	44.88	1.12	−2.07	422.56	−0.06658	0.27	1.06	11.41
12	1032	640	15.9	33.69	0.79	−4.94	536.49	0.16531	0.17	1.41	6.9
13	1065	660	31.07	43.71	2.11	−6.66	587.7	0.123019	0.44	2.89	15.55
14	4032	2500	12.6	18.47	0.92	−20.24	1163.9	0.814388	0.13	10.23	10.36
15	1258	780	27.34	40.77	1.63	−6.24	522.98	0.442393	0.36	3.145	14.14
16	1290	800	23.47	35.72	1.42	−7.78	586.1	0.454105	0.29	3.6	32.52
17	1694	1050	50.4	64.61	3.72	−2.71	350.6	0.093731	0.99	3.05	48.34
18	1097	680	31.17	45.58	1.89	−5.09	476.37	0.139142	0.43	2.6	31.06
19	2710	1680	36.18	45.32	3.1	−10.1	779.27	0.298076	0.55	4.45	15.83
20	1855	1150	48.37	59.33	3.87	−4.56	440.85	0.292737	0.92	4.31	17.43
21	1855	1150	37.83	58.64	1.78	−1.46	249.59	−1.57224	0.56	1.56	41.28

(continued)

Table 4 (continued)

Sample number	EC	TDS	SC	PI	SAR	RSC	Hardness	CAI	KI	CR	MH
22	1375	880	67.47	75.36	7.17	−3.78	307.34	−0.05054	2.04	9.16	33.65
23	1540	985.6	45.62	51.63	4.68	−12.55	800.58	−0.99662	0.83	8.48	14.95
24	1420	908.8	50.16	55.94	4.91	−10	612.4	0.249859	0.99	12.86	26.41
25	470	216.2	19.06	38.02	0.79	−3.94	350.85	−1.13901	0.21	1.97	20.45
26	764	488.9	86.57	107.68	10.06	2.92	63.49	−3.79013	6.29	1.64	49.99
27	470	300.8	23.13	24.19	1.59	−14.93	748.5	0.169778	0.29	189.19	33.21
28	518	331.5	24.79	42.74	1.21	−3.8	389.04	−1.71418	0.31	1.76	15.38
29	477	305	27.49	47.41	1.3	−2.88	337.34	−0.19424	0.35	1.69	30.67
30	481	307	73.06	95.78	4.88	0.95	86.89	−1.06646	2.61	1.8	43.42
31	824	527.8	78.95	97.05	7.67	1.46	109.23	−2.42152	3.66	2.18	43.63
32	650	416	72.39	86.16	5.56	−0.4	118.88	−0.82695	2.54	4.16	58.32
33	1280	819	78.84	90.02	9.28	0.26	158.85	−0.66116	3.67	4.31	45
34	874	559	100	129.24	6.3	3.4	0	−2.63594	3.15	0.64	50
35	990	633.6	46.89	62.24	1.62	−1.43	87.68	−0.49298	0.86	10.38	46.22
36	490	313.6	46.55	60.53	2.7	−3.15	258.37	−1.58594	0.84	4.24	39.22
37	888	568.3	50.55	64.02	3.83	−2.11	371.44	−0.17637	0.99	2.54	1.08
38	1070	684.8	77.84	89.72	9	0	169.04	−2.32945	3.45	4.36	35.28
39	872	558	62.71	77.6	4.61	−1.3	199.04	−2.25532	1.63	3.39	29.99
40	430	275.2	31.31	55.43	1.23	−1.16	219.1	−1.79493	0.42	0.88	25.45
41	400	245.8	12.52	47.96	0.29	−1.36	166.99	0.284261	0.11	1.09	34.48
42	400	245.8	16.71	52.39	0.44	−1.2	159.2	−0.11811	0.17	1.07	31.24

(continued)

Table 4 (continued)

Sample number	EC	TDS	SC	PI	SAR	RSC	Hardness	CAI	KI	CR	MH
43	500	336.6	5.09	34.86	0.1	−2.33	248.23	0.766878	0.03	1.18	33.88
44	1100	678.4	9.46	22.67	0.4	−7.38	476.99	0.724609	0.09	4.57	38.1
45	800	529.3	2.51	22.46	0.07	−5.17	399.72	0.913316	0.02	2.26	50.86
46	2600	1676.8	10.6	18.87	0.78	−18.32	1163.07	0.694855	0.11	4.99	43.64
47	700	434.6	22.25	45.46	0.87	−2.62	263.12	0.368665	0.27	1.96	20.83
48	1200	761.6	26.04	42.41	1.43	−4.8	439.12	0.281233	0.34	2.48	12.5
49	2900	1843.2	50	55.79	5.34	−11.51	715.79	−0.20286	0.99	10.96	35.82
50	500	313	25.41	58.25	0.87	−0.98	181	0.136008	0.32	1.08	45.69
51	800	498.6	38.37	63.56	1.86	−0.8	238.53	−0.04059	0.6	1.27	40.42
52	400	255.4	13.35	45.01	0.31	−1.68	171.57	0.536268	0.12	1.55	42.68
53	300	222.7	44.81	82.53	1.47	−0.14	95.52	−0.25141	0.75	1.27	31.24
54	400	260.5	5.61	36.75	0.09	−2.07	190.5	0.816558	0.03	1.62	54.2
55	300	222.7	11.71	48.71	0.26	−1.29	152.1	0.613588	0.1	1.23	56.99
56	2000	1288.4	57.03	65.02	5.48	−5.97	428.62	−0.89961	1.32	7.69	46.5
57	1700	1055	59.29	67.65	5.28	−4.72	333.71	−1.269	1.44	8.39	41.05
Minimum value	**300**	**216.2**	**2.51**	**18.47**	**0.07**	**−20.24**	**63.49**	**−6.67**	**0.018**	**0.46**	**1.08**
Maximum value	**4032**	**2500**	**100**	**129.24**	**10.06**	**6.52**	**1163.9**	**0.913**	**6.29**	**189.19**	**58.32**
Average value	**1127.83**	**709.08**	**39.53**	**57.24**	**3.02**	**−3.91**	**391.15**	**−0.66**	**1**	**6.61**	**31.26**
Standard deviation	**734.6**	**458.9**	**23.56**	**23.67**	**2.6**	**6.42**	**258.94**	**1.52**	**1.21**	**24.56**	**14.95**

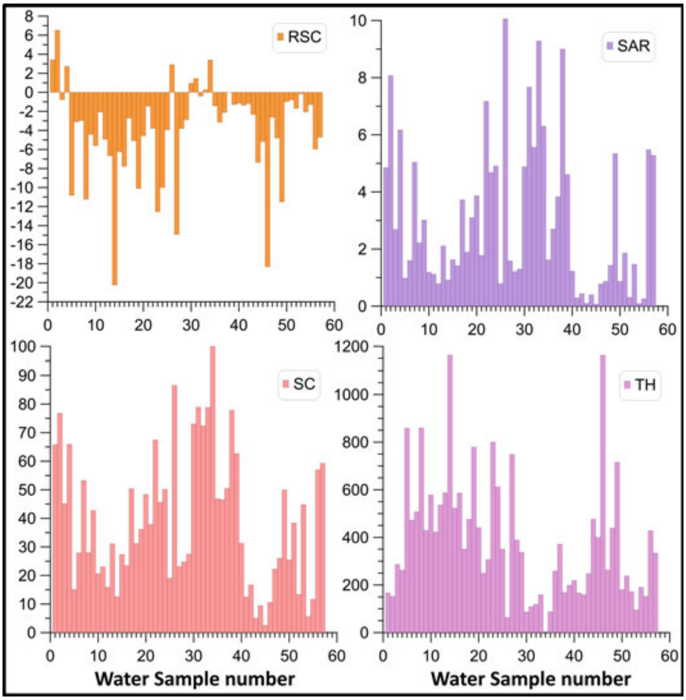

Fig. 14 Bar chart plots represent different water quality parameters

in lowering the soil ability to construct stable aggregates and soil structure loss (Şen 2015).

6.3 Residual Sodium Carbonate (RSC)

RSC evaluates the risk effect on the groundwater caused by excess concentration of both bicarbonate and carbonate (Raju 2007). High content of HCO_3^- results in the precipitation of both Ca^{2+} and Mg^{2+} as CO_3^{2-}, therefore soil would be enriched with Na^+. RSC influences the electric conductivity, alkalinity, and SAR (Naseem et al. 2010). RSC values would be estimated by Eq. 6 (Şen 2015):

$$RSC = \left(CO_3^{2-} + HCO_3^{-}\right) - \left(Ca^{2+} + Mg^{2+}\right) \quad (6)$$

all concentrations are in meq/L.

6.4 Permeability Index (PI)

Permeability index (PI) is important to deduce the groundwater appropriateness for irrigation aims. Water content of calcium, sodium, bicarbonates and magnesium influences by long term use the permeability of the soil. Doneen (1962) has calculated PI value using Eq. 7 where ions are in meq/L.

$$PI = 100 * \frac{Na^{+} + \sqrt{HCO_3^-}}{Ca^{2+} + Mg^{2+} + Na^{+}} \quad (7)$$

6.5 EC and SAR Relationship

EC together with SAR are good indicators for the availability of groundwater for cultivation purposes. SAR and EC data could be exhibited using a USSL (1954) diagram to decide the validity of water for irrigation (Fig. 15). The USSL diagram shows EC on the horizontal versus SAR on the vertical axes. USSL diagram reveals that about 93% of the water samples show a wide range of both salinity and alkalinity having the following types C2S1, C3S1 and C3S2. These types reveals that the groundwater types are good to excellent depending on the sodium hazard class and are good to doubtful depending on the salinity hazard, while the rest of samples: S14, S19, S46 and S49 are not suitable for irrigation because they are classified as C4S3 and C4S4 (see Fig. 16 to see the locations of these samples).

6.6 Magnesium Hazard (MH)

Generally, both calcium and magnesium ions are found in equilibrium state in groundwater (Negm and Armanuos 2017). High levels of Mg^{2+} in water cause converting the quality of soils to alkaline and reducing the crops. Szabolcs and Darab (1964) suggested an index expresses the water suitability for irrigation purposes, this parameter is known as magnesium hazard (MH) which is given by Eq. 8:

$$MH = Mg^{2+} / \left(Ca^{2+} + Mg^{2+}\right) \times 100 \quad (8)$$

where Mg^{2+} and Ca^{2+} concentrations are in meq/L.

When MH exceeds 50%, then groundwater would be harmful and unsuitable for irrigation aims. Generally, groundwater samples are classified based on MH ratio (Table 3) to be suitable for irrigation goals (89.48%), whereas only 10.52% of the samples (boreholes 1, 2, 32, 45, 54, and 55) are classified as unsuitable for the agricultural purposes (refre to Table 4).

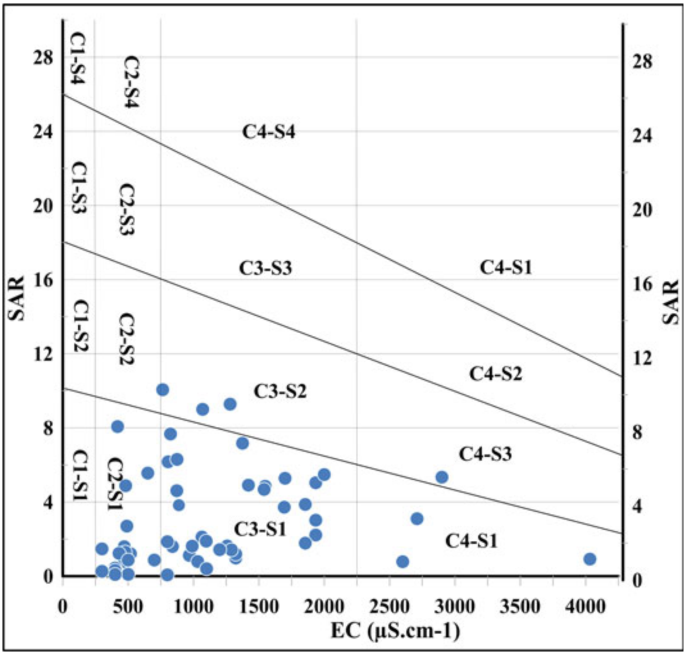

Fig. 15 SAR-EC water classification diagram for irrigation purposes

6.7 Kelly's Ratio (KI)

Kelly's ratio is also a parameter that indicates the validity of groundwater for agricultural activities. This ratio is expressed by the following formula (Negm and Armanuos 2017):

$$KI = Na^{+}/\left(Ca^{2+} + Mg^{2+}\right) \tag{9}$$

where Ca^{2+}, Na^{+}, and Mg^{2+} concentrations are in meq/L.

According to Narsimha et al. (2013) and according to the calculated KI values, groundwater would be grouped into suitable water for irrigation purposes (KI < 1) representing 73.7% of the groundwater samples, while 26.3% of the samples are unsuitable water (KI > 1).

6.8 Chloride Classification

Chloride concentration in groundwater is affected by agricultural activities, and human and animal waste sources because Cl^{-} is well transported through the soil (Stallard and Edmond 1981). Stuyfzand (1989) has classified groundwater based

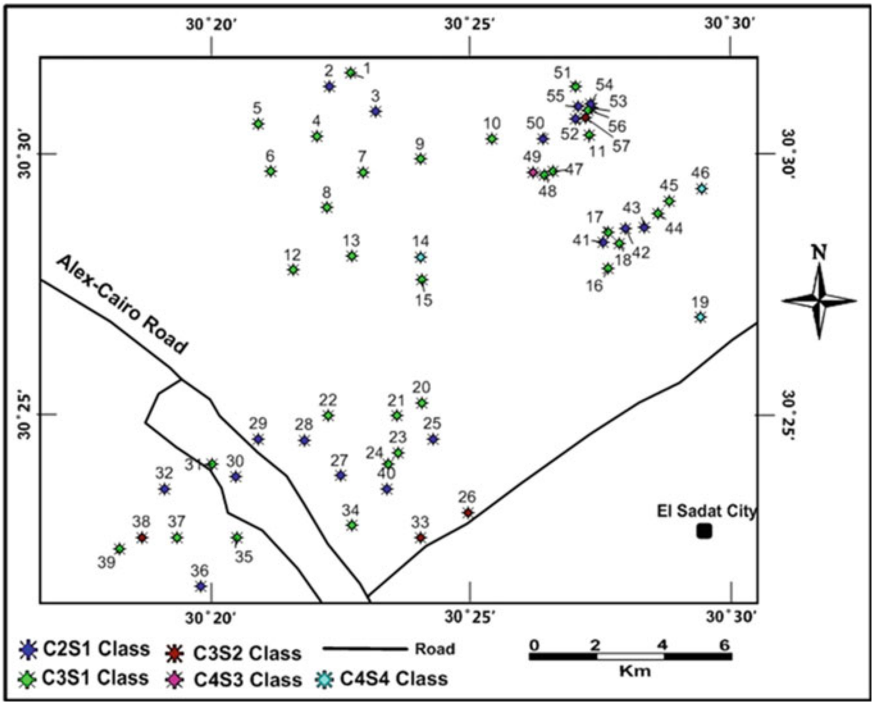

Fig. 16 Spatial distribution map for the types revealed from SAR-EC water classification diagram

on Cl^- concentration in meq/L into: hypersaline, salt, brackish-salt, brackish, fresh-brackish, fresh, very fresh and extremely fresh. Thus, our groundwater samples are grouped into: very fresh water (61.4%), fresh-brackish water (22.8%), and brackish water (15.8%).

6.9 Chloro-Alkaline Indices (CAI)

This index denotes the aquifer's ion exchange phase which occurs between the soil and the groundwater. CAI is expressed by Eq. 10 (Schoeller 1967).

$$\text{CAI} = \frac{Cl^- - (Na^+ + K^+)}{Cl^-} \qquad (10)$$

Based on CAI values; negative values refer to ion exchange phase between K^+ and Na^+ in groundwater and Mg^{2+} and Ca^{2+} in the rock (Negm and Armanuos 2017). By calculating the CAI values, it could be concluded that 57.9% of water samples has negative CAI values (Table 4) and this is emphasized by Durov diagram.

6.10 *Corrosively Ratio (CR)*

Corrosively ratio (CR) is an index reflecting the safety for groundwater transportation in metallic pipes (Negm and Armanuos 2017). If this ratio is less than 1, this means that it is safe to transport groundwater in any type of pipes, otherwise if it is higher than 1, this refers to the corrosive nature of the groundwater and it would be not safe to transport water through metal pipes. This index is given by Eq. 11:

$$CR = \left(\frac{Cl^{-}}{35.5} + 2\frac{SO_4{}^{2-}}{96}\right)/2\left(\frac{HCO_3{}^{-} + CO_3{}^{2-}}{100}\right) \tag{11}$$

All anions' concentrations are in meq/L unit.

In accordance with the calculated CR values (Table 4), it would be deduced that the CR values of almost water samples are greater than 1, so it is unsafe to transport this water in metal pipes for long distances.

7 Results and Discussion

Hydrochemistry has an incredible significance in quality assurance and characterization of groundwater, and subsequently, choice if this water is appropriate for various demands, for example, drinking, household, cultivation, and industrial purposes. Depending on the groundwater analysis of 57 collected samples from several drilled boreholes in the surveyed region, important information about the concentrations of both major anions and cations, Fe–Mn trace elements, furthermore TDS and EC are obtained. Groundwater reasonableness to use for drinking and irrigation was assessed depending on the realized standard values of the guidelines.

Several numerical indicators including EC, TDS and TH have been studied. EC concentrations range between 300 and 4032 μS/cm with the value of 1127.83 μS/cm on average. As a result, groundwater in the examined region could be divided into permissible water (59.65%) and good water (33.33%) categories, with just 3 water samples categorised as doubtful (boreholes 19, 46, 49). Only one sample from borehole 14 was declared unsuitable for drinking. Concerning TDS level, when TDS level in the water samples is beneath 600 mg/L, the groundwater would be suitable for drinking while the threshold limit is 1000 mg/L (WHO 2011). TDS values change between 216 and 2500 mg/L with an average value of 709 mg/L. Most of the water samples collected from the study area are categorized into freshwater (79.31%, their TDS < 1000 mg/L), except 12 samples represent brackish water (21.05%). Furthermore, it is worth mentioning that groundwater having TDS values below 600 mg/L represents 50.88% of the existing samples.

Distribution maps of TDS, EC and TH exhibit a high EC and TDS level zone at the northwestern part. It is also obvious that there are moderate concentration zones in the central (extending NW–SE) and eastern regions at the studied area, while the lowest levels, on the other hand, are clustered towards the southwest. This might be resulted from different reasons such as recharge decrease from the Rosetta branch and/or increase discharge process for agricultural drainage. Moreover, EC has a strong relation with TDS, TH, Ca^{2+}, Cl^{-}, Na^{+} and intermediate linkage with HCO_3^{-}, SO_4^{2-}, Mg^{2+} indicating that such cations and anions have an identical source and are implicated in the reactions of ion exchange (Rao 2002). Furthermore, TDS has high correlations with Ca^{2+}, Mg^{2+}, and Na^{+}. As EC could be estimated directly in the field; hence, TDS level can be computed by using the obtained formula (Eq. 2). Hence, with great benefits such as saving time, money, and efforts, an economic study of water quality can be carried out using this equation.

Groundwater's total hardness reveals that the maximum concentration is 1163 mg/L at well 46 where there are some high contents of Mg^{2+} and Ca^{2+} (264 and 122.7 mg/L; respectively), while the minimum value is 63 mg/L at well 26 this corresponds low concentrations of Ca^{2+} (12.8 mg/L) and Mg^{2+} (7.68 mg/L). The average hardness value is 391 mg/L. According to hardness levels, groundwater is grouped into soft (3.51%), moderately hard (8.77%), hard (33.33%), and very hard (54.39%) waters (Tables 1 and 4). TH is highly related to Mg^{2+}, Ca^{2+}. This analysis suggests that the groundwater in the study area is rich with Mg^{2+} and Ca^{2+} salts. From the previous numerical indicators, it could be extracted that most of the groundwater is suggested to be fresh to brackish water and suitable for drinking and domestic utilities.

Groundwater quality for agricultural purposes was evaluated based on several indicators such SC, PI, SAR, RSC, MH, Kelly's ratio, and chloride classification. These indicators suggest suitable and safe groundwater for agricultural activities (Tables 3 and 4). SC is a very significant index for agriculture purposes. Based on Wilcox (1955) classification, groundwater is categorized into good to excellent water (54.39% of the samples), permissible water (24.56% of water samples), while 17.54% is doubtful water for irrigation, but 3.51% of the samples (found at boreholes no. 26 and 34) are not suited for irrigation as SC exceeds 80%. The estimated groundwater SAR values change from 0.07 to 10.06 epm. So, it is worth to conclude that the groundwater in the research region is ideal for irrigation aims for all types of soils with very low sodium hazards.

Based on RSC values, generally groundwater in the study area is suitable for both drinking and irrigation purposes. 91.13% of the water has RSC less than1.25 while 8.77% exceeds the acceptable value (2.5 mg/L) at five boreholes (1, 4, 2, 26, and 34) that suggests the unsuitability of the water for irrigation purposes (Eaton 1950; Richards 1954). Another classification of groundwater is depending on PI values. This classification is subdivided into three classes: I, II, and III. Naseem et al. (2010) mentioned classes I and II when the highest permeability is 75% or more, then groundwater is good for irrigation, furthermore class III is obtained when the highest permeability is 25% and this causes the unsuitability of the groundwater for irrigation. Calculated values of PI reveal that classes I and II account 91.23% of the samples, indicating the suitability of the groundwater for irrigation. However, 8.77% of the water samples override the PI limits and are described as unsuitable water. This only applies to five groundwater samples at boreholes 14, 27, 44, 45, and 46.

Both electrical conductivity and the sodium concentration (%) are commonly used to describe the groundwater quality for agricultural needs (Yidana et al. 2010). Representing EC versus SAR values on the USSL diagram reveals that 93% of groundwater samples are of the following types C2S1, C3S1 and C3S2, which indicates that these waters are good to excellent based on the sodium hazard class and these waters also are good to doubtful depending on the salinity hazard. Moreover, about 7% of the samples (S14, S19, S46 and S49) are not suitable for irrigation purposes as they are classified as C4S3 and C4S4.

8 Conclusions

Results obtained from the hydrochemical interpretation show a clear harmony deduced from EC, TDS, and TH distribution maps. In the northwest part, it appears to have high values of EC, TDS, and TH. Moreover, cations distribution maps present high values at the same area. Therefore, this part is somehow not suitable for domestic purposes but could be used for agriculture utilities with some restrictions. The rest regions of the area have moderate to low values of EC, TDS, TH, cations, and anions levels. Hence, at these areas, waters are good for the different uses. In majority of the boreholes, the EC and TDS readings indicate fresh to brackish water, while the hardness indicates hard to extremely hard water. The hydrochemical outcomes were correlated with the levels of well-known standard guidelines. Water types in the area are classed as follows based on the amounts of major ions: Ca–HCO_3 (22.81%), Ca–SO_4 (17.54%), Na–SO_4 (15.79%), Na–Cl (14.03%), Ca–Cl (14.03%), Na–HCO_3 (10.53%), Mg–HCO_3 (3.51%), and Mg–SO_4 (1.75%). The research area's groundwater is characterised by a high concentration of alkaline earth and strong acids. Also, the cations and anions have mostly the same source and are implicated in the ion exchange reactions. Different water quality indicators such as SC, SAR, MH, PI, and RSC recommend safe and proper groundwater for agricultural objectives.

9 Recommendations

The southern, central, and eastern parts of the study area are thought to be the best locations for future water supply boreholes. However, prior to any process of groundwater exploitation in such favorable district, excessive research should be considered to control the basis for groundwater abstraction in order to avoid potential difficulties related with excessive groundwater abstraction. This involves e.g. groundwater age dating using isotopes, recognizing and distinguishing areas of recharge, and simulating the impact of various groundwater abstraction scenarios. Moreover, it is important to detect the recharge areas to protect them and avoid pollution problem of the aquifer.

References

Abd El-Kawy OA, Rød JK, Ismail HA, Suliman AS (2011) Land use and land cover change detection in the western Nile delta of Egypt using remote sensing data. Appl Geogr 31:483–494

Abdel Aal A, Price R, Vaitl J, Shrallow J (1994) Tectonic evolution of the Nile delta, its impact on sedimentation and hydrocarbon potential. EGPC 12:19–34

Abdel Aal A, El Barkooky A, Gerrits M, Meyer HJ, Schwander M, Zaki H (2001) Tectonic evolution of the eastern Mediterranean basin and its significance for the hydrocarbon prospectivity of the Nile delta deepwater area. GeoArabia 6:363–384

Abdel Baki AA (1983) Hydrogeological and hydrogeochemical studies in the area west of Rosetta branch and south of El Nasr canal. Ph.D. thesis, Faculty of Science, Ain Shams University, Cairo, Egypt, p 156

Abd-Elhamid H, Abdelaty I, Sherif M (2019) Evaluation of potential impact of Grand Ethiopian Renaissance Dam on seawater intrusion in the Nile delta aquifer. Int J Environ Sci Technol 16(5):2321–2332

Aghazadeh N, Mogaddam AA (2010) Assessment of groundwater quality and its suitability for drinking and agricultural uses in the Oshnavieh area, northwest of Iran. J Environ Prot 1:30

Ahmed S (1999) Hydrological and isotope assessment of groundwater in Wadi El-Natrun and Sadat city, Egypt. Ain Shams University, Cairo, p 237

Ahmed MA, Samie SA, El-Maghrabi HM (2011) Recharge and contamination sources of shallow and deep groundwater of Pleistocene aquifer in El-Sadat industrial city: isotope and hydrochemical approaches. Environ Earth Sci 62(4):751–768

Al-Bassam AM, Awad HS, Al-Alawi JA (1997) Durov plot: a computer program for processing and plotting hydrochemical data. Ground Water 35(2):362–367

Al-Kilany S (2001) A new geoelectrical studies on groundwater aquifer, El-Sadat area and its vicinities Egypt. Dissertation, Menoufiya University, Egypt

Appelo CAJ, Postma D (1996) Geochemistry groundwater and pollution. Balkema, Rotterdam

Atta S, Sharaky A, El Hassanein A, Khallaf K (2005) Salinization of the groundwater in the coastal shallow aquifer, northwestern Nile delta, Egypt. In: First international conference on the geology of Tethys, Cairo University, pp 151–166

Attwa M, Ali H (2018) Resistivity characterization of aquifer in coastal semiarid areas: an approach for hydrogeological evaluation. In: Groundwater in the Nile delta. Springer, Cham, pp 213–233

Bartarya S (1993) Hydrochemistry and rock weathering in a sub-tropical lesser Himalayan river basin in Kumaun, India. J Hydrol 146:149–174

Burbery L, Vincent C (2009) Hydrochemistry of south Canterbury tertiary aquifers. Environment Canterbury. Christchurch, New Zealand

Chow VT (1964) Handbook of Applied Hydrology. Sec. 11: Evapotranspiration. Mc-Graw Hill Co., New York, pp 11–38

Dauda M, Habib G (2015) Graphical techniques of presentation of hydro-chemical data. J Environ Earth Sci 5:65–76

Dawoud MA, Darwish MM, El-Kady MM (2005) GIS-based groundwater management model for western Nile delta. Water Resour Manage 19(5):585–604

Doneen LD (1962) The influence of crop and soil on percolating water. In: Proceeding 1961 biennial conference on groundwater recharge, pp 156–163

Durov S (1948) Natural waters and graphic representation of their composition. Dokl Akad Nauk SSSR 59:87–90

Eaton FM (1950) Significance of carbonates in irrigation waters. Soil Sci 69(2):123–134

Edmunds W, Cook J, Darling W, Kinniburgh D, Miles D, Bath A, Morgan-Jones M, Andrews J (1987) Baseline geochemical conditions in the Chalk aquifer, Berkshire, UK: a basis for groundwater quality management. Appl Geochem 2:251–274

El Abd E (2005) The geological impact on the water bearing formations in the area southwest Nile delta, Egypt. Unpublished PhD thesis, Faculty of Science, Menufiya University, Egypt

El Kashouty M, El Sabbagh A (2011) Distribution and immobilization of heavy metals in Pliocene aquifer sediments in Wadi El Natrun depression, Western Desert. Arab J Geosci 4:1019–1039
El Osta M, Hussein H, Tomas K (2018) Numerical simulation of groundwater flow and vulnerability in Wadi El-Natrun depression and vicinities, west Nile delta, Egypt. J Geol Soc India 92(2):235–247
ElGalladi A, Ghazala HH, Ibraheem IM, Ibrahim E-K (2009) Tectonic interpretation of gravity field data of west of Nile delta region, Egypt. NRIAG J Astron Geophys Egypt Spec Issue 487–508
Embaby A (2003) Environmental evolution for geomorphological situation in relation to the water and soil resources of the region north of the Sadat city, west Nile delta, Egypt. Unpublished Ph.D. thesis, Faculty of Science, Mansoura University, Egypt, vol 60, p 323
Fetter CW (2014) Applied hydrogeology, 4th edn. Pearson, UK, p 604
Gaber A, Mohamed AK, ElGalladi A, Abdelkareem M, Beshr AM, Koch M (2020) Mapping the groundwater potentiality of West Qena Area, Egypt, using integrated remote sensing and hydro-geophysical techniques. Remote Sens 12(10):1559
Gad M, El-Hendawy S, Al-Suhaibani N, Tahir MU, Mubushar M, Elsayed S (2020) Combining hydrogeochemical characterization and a hyperspectral reflectance tool for assessing quality and suitability of two groundwater resources for irrigation in Egypt. Water 12(8):2169
Garfunkel Z (1998) Constrains on the origin and history of the eastern Mediterranean basin. Tectonophysics 298:5–35
Geirnaert W, Laeven M (1992) Composition and history of ground water in the western Nile delta. J Hydrol 138:169–189
Ghoraba SM, Khan AD (2013) Hydrochemistry and groundwater quality assessment in Balochistan province, Pakistan. Int J Res Rev Appl Sci 17(2):185–199
Guiraud R, Bosworth W (1999) Phanerozoic geodynamic evolution of northeastern Africa and the northwestern Arabian platform. Tectonophysics 315:73–104
Harms JC, Wray JL (1990) Nile delta. In: Said R (ed) The geology of Egypt. Balkema, Rotterdam, Netherlands
Heath RC (1983) Basic groundwater hydrology. US geological survey water supply paper 2220. US Geological Survey. https://doi.org/10.3133/wsp2220
Hegazy D, Abotalib AZ, El-Bastaweesy M, El-Said MA, Melegy A, Garamoon H (2020) Geo-environmental impacts of hydrogeological setting and anthropogenic activities on water quality in the Quaternary aquifer southeast of the Nile delta, Egypt. J Afr Earth Sci 172:103947
Hopkins BG, Horneck DA, Stevens RG, Ellsworth JW, Sullivan DM (2007) Managing irrigation water quality for crop production in the Pacific Northwest. [Covallis, Or.]: Oregon State University Extension Service
Hudson RO, Golding DL (1997) Controls on groundwater chemistry in subalpine catchments in the southern interior of British Columbia. J Hydrol 201(1–4):1–20
Ibraheem IM (2009) Geophysical potential field studies for developmental purposes at El-Nubariya–Wadi El-Natrun, west Nile delta, Egypt. Ph.D thesis, Faculty of Science, Mansoura University, Egypt, p 193
Ibraheem IM, El-Qady G (2017) Hydrogeophysical investigations at El-Nubariya–Wadi El-Natrun area, west Nile delta, Egypt. In: The handbook of environmental chemistry. Springer, Berlin, Heidelberg. https://doi.org/10.1007/698_2017_154
Ibraheem IM, El-Qady G (2019) Hydrogeophysical investigations at El-Nubariya–Wadi El-Natrun area, west Nile delta, Egypt. In: Negm A (ed) Groundwater in the Nile delta. The handbook of environmental chemistry, vol 73. Springer, Cham, pp 235–271
Ibraheem IM, El-Qadi GM, ElGalladi A (2016) Hydrogeophysical and structural investigation using VES and TDEM: a case study at El-Nubariya–Wadi El-Natrun area, west Nile delta, Egypt. NRIAG J Astron Geophys 5(1):198–215
Ibraheem IM, Elawadi EA, El-Qady GM (2018) Structural interpretation of aeromagnetic data for the Wadi El Natrun area, northwestern desert, Egypt. J Afr Earth Sci 139:14–25
Jacks G (1973) Chemistry of ground water in a district in southern India. J Hydrol 18:185–200

Karanth KR (1991) Impact of human activities on hydrogeological environment. J Geol Soc India 38(2):195–206

Kimblin RT (1995) The chemistry and origin of groundwater in Triassic sandstone and Quaternary deposits, northwest England and some UK comparisons. J Hydrol 172(1–4):293–308

Lloyd JW, Heathcote JA (1985) Natural inorganic hydrochemistry in relation to groundwater: an introduction. Oxford University Press, New York, p 296

Massoud U, Kenawy AA, Ragab ES, Abbas AM, El-Kosery HM (2014) Characterization of the groundwater aquifers at El Sadat city by joint inversion of VES and TEM data. NRIAG J Astron Geophys 3:137–149

Mayo AL, Loucks MD (1995) Solute and isotopic geochemistry and groundwater flow in the central Wasatch Range, Utah. J Hydrol 172(1–4):31–59

McCool JP (2019) Carbonates as evidence for groundwater discharge to the Nile river during the Late Pleistocene and Holocene. Geomorphology 331:4–21

Menco (1990) Miser company for engineering and agricultural projects report

Miller JA (1991) Summary of the hydrology of the southeastern coastal plain aquifer system in Mississippi, Alabama, Georgia, and South Carolina. U.S. Geol Surv Prof 1410-A:33–36

Mohamed A (2020) Gravity applications to groundwater storage variations of the Nile delta aquifer. J Appl Geophys 104177

Mohamed RF, Hua CZ (2010) Regional groundwater flow modeling in western Nile delta, Egypt. World Rural Obs 2:37–42

Mosaad S, Basheer AA (2020) Utilizing the geophysical and hydrogeological data for the assessment of the groundwater occurrences in Gallaba plain, western desert, Egypt. Pure Appl Geophys 1–22

Narsimha A, Sudarshan V, Swathi P (2013) Groundwater and its assessment for irrigation purpose in Hanmakonda area, Warangal district, Andhra Pradesh, India. Int J Res Chem Environ 3(2):196–200

Naseem S, Hamza S, Bashir E (2010) Groundwater geochemistry of Winder agricultural farms, Balochistan, Pakistan and for irrigation water quality. Eur Water 31:21–32

Negm AM, Armanuos AM (2017) GIS-based spatial distribution of groundwater quality in the western Nile delta, Egypt. In: Negm AM (ed) The Nile delta. Springer, Cham, pp 89–119

Omara SM, Sanad S (1975) Rock stratigraphy and structural features of the area between Wadi El Natrun and the Moghra depression, Western Desert, Egypt. Geol J Hannover 16:45–73

Othman A, Ibraheem IM, Ghazala H, Mesbah H, Dahlin T (2019) Hydrogeophysical and hydrochemical characteristics of Pliocene groundwater aquifer at the area northwest El Sadat city, west Nile delta, Egypt. J Afr Earth Sci 150:1–11

Patil VB, Pinto SM, Govindaraju T, Hebbalu VS, Bhat V, Kannanur LN (2020) Multivariate statistics and water quality index (WQI) approach for geochemical assessment of groundwater quality—a case study of Kanavi Halla sub-basin, Belagavi, India. Environ Geochem Health 1–18

Piper AM (1944) A graphic procedure in the geochemical interpretation of water-analyses. EOS Trans Am Geophys Union 25(6):914–928

Piper AM (1953) A graphic procedure in the geochemical interpretation of water analysis. US department of the interior, geological survey. Water Resources Division, Ground Water Branch, Washington

Raju NJ (2007) Hydrogeochemical parameters for assessment of groundwater quality in the upper Gunjanaeru River basin, Cuddapah district, Andhra Pradesh, South India. Environ Geol 52(6):1067–1074

Rao NS (2002) Geochemistry of groundwater in parts of Guntur district, Andhra Pradesh, India. Environ Geol 41(5):552–562

Richards LA (1954) Diagnosis and improvement of saline and alkali soils. Handbook, vol 60. U.S. Department of Agriculture, Washington, DC, p 160

RockWare Inc. (2004) A user's guide to RockWare® Aq·QA®, version 1.1. RockWare, Inc. Golden, Colorado, USA

Rogers RJ (1989) Geochemical comparison of ground water in areas of New England, New York, and Pennsylvania. J Groundwater 27(5):690–712

Sadek HS, Soliman SA, Abdulhadi HM (1990) A correlation between the different models of resistivity sounding data to discover a new fresh water field in El Sadat city, western desert of Egypt. In: Geophysical data inversion methods and applications. Vieweg + Teubner Verlag, Wiesbaden, pp 329–346

Said R (1962) The geology of Egypt. Elsevier, Amsterdam

Salem ZE, El-Bayumy DA (2016) Hydrogeological, petrophysical and hydrogeochemical characteristics of the groundwater aquifers east of Wadi El-Natrun, Egypt. NRIAG J Astron Geophys

Salem ZE, Osman OM (2017) Use of major ions to evaluate the hydrogeochemistry of groundwater influenced by reclamation and seawater intrusion, west Nile delta, Egypt. Environ Sci Pollut Res 24(4):3675–3704

Salem ZE, Gaame OM, Hassan TM (2018) Integrated subsurface thermal regime and hydrogeochemical data to delineate the groundwater flow system and seawater intrusion in the middle Nile delta, Egypt. In: Groundwater in the Nile delta. Springer, Cham, pp 461–486

Salem ZE, Sefelnasr AM, Hasan SS (2019) Assessment of groundwater vulnerability for pollution using DRASTIC index, young alluvial plain, western Nile delta, Egypt. Arab J Geosci 12(23):727

Salomons W, Forstner U (1984) Metals in the hydrocycle. Springer-Verlag, Berlin, p 349

Sarhan M, Hemdan K (1994) North Nile delta structural setting and trapping mechanism, Egypt. In: Proceedings of the 12th petroleum conference of EGPC, vol 12, pp 1–17

Sarhan M, Barsoum F, Bertello F, Talaat M, Nobili M (1996) The Pliocene play in the Mediterranean offshore: structural setting and growth faults-controlled hydrocarbon accumulations in the Nile delta basin. A comparison with the Niger delta basin. In: 13th EGPC, Egyptian general petroleum corporation conference, vol 1, Cairo, pp 1–19

Sayyed A, Bhosle B (2011) Analysis of chloride, sodium and potassium in groundwater samples of Nanded City in Mahabharata, India. Europ J Exp Biol 1:74–82

Schoeller H (1967) Geochemistry of groundwater. An international guide for research and practice, chap 15. UNESCO, pp 1–18

Şen Z (2015) Practical and applied hydrogeology. Elsevier, p 407

Sharaky AM, Atta SA, El Hassanein AS, Khallaf KM (2007) Hydrogeochemistry of groundwater in the western Nile delta aquifers, Egypt. In: 2nd international conference on the geology of Tethys, vol 1, pp 1–23

Sharaky AM, El Hasanein AS, Atta SA, Khallaf KM (2017) Nile and groundwater interaction in the Western Nile Delta, Egypt. In: Negm AM (ed) The Nile Delta. Springer, Cham, pp 33–62

Shata A (1953) New light on the structural development of the western desert of Egypt. Bull Inst Desert Egypt 6:117–157

Shata A (1955) An introductory note on the geology of the northern portion of the western desert of Egypt. Bull Inst Desert Egypt 5(3):87–98

Shata A (1959) Geological problems related to the groundwater supply of some desert areas of Egypt. Bull Soc Geogr Egypt 32:247–262

Shata A (1961) The geology of groundwater supplies in some arable lands in the desert of Egypt. Desert Institute, Cairo, Egypt

Shedid A (1989) Geological and hydrogeological studies of El Sadat area and its vicinities. MSc thesis, Faculty of Science, El Menoufia University, Shibin El Kom, Cairo, Egypt, p 157

Sherif M (1999) Nile delta aquifer in Egypt. In: Seawater intrusion in coastal aquifers—concepts, methods and practices. Springer

Stallard R, Edmond J (1981) Geochemistry of the Amazon: 1. Precipitation chemistry and the marine contribution to the dissolved load at the time of peak discharge. J Geophys Res 86:9844–9858

Stallard R, Edmond J (1983) Geochemistry of the Amazon: 2. the influence of geology and weathering environment on the dissolved load. J Geophys Res Oceans 88:9671–9688

Stimson J, Frape S, Drimmie R, Rudolph D (2001) Isotopic and geochemical evidence of regional-scale anisotropy and interconnectivity of an alluvial fan system, Cochabamba Valley, Bolivia. Appl Geochem 16(9–10):1097–1114

Stuyfzand PJ (1989) Hydrology and water quality aspects of Rhine bank groundwater in the Netherlands. J Hydrol 106(3–4):341–363

Szabolcs I, Darab C (1964) The influence of irrigation water of high sodium carbonate content on soils. Agrokém Talajt 13:237–246

Todd DK, Mays LW (2005) Groundwater hydrology, 3rd edn. Wiley, Hoboken, NJ, p 891

USL Staff (1954) Diagnosis and improvement of saline and alkali soils. In: Agriculture handbook, vol 60, pp 83–100

Walton NRG (1989) Electrical conductivity and total dissolved solids—what is their precise relationship? Desalination 72(3):275–292

Wilcox LV (1955) Classification and use of irrigation waters. Circ. 969. US Department of Agriculture, Washington, DC, p 19

World Health Organization (WHO) (2011) Guidelines for drinking-water quality, vol 216. World Health Organization, pp 303–304

Yidana SM, Banoeng-Yakubo B, Akabzaa TM (2010) Analysis of groundwater quality using multivariate and spatial analyses in the Keta basin, Ghana. J Afr Earth Sci 58(2):220–234

Zaghloul Z (1976) Stratigraphy of the Nile delta. In: Proceedings of the seminar on Nile delta sedimentology, pp 40–49

Zaporozec A (1972) Graphical interpretation of water quality data. Groundwater 10(2):32–43